International Journal of Engineering and Geosciences
https://dergipark.org.tr/en/pub/ijeg
e-ISSN 2548-0960

UAV-mounted thermal camera and its analysis on urban surface textures

Efdal Kaya [*1], **Arzu Erener** [2]

[1] *Iskenderun Technical University, City and Region Planning, Türkiye, efdal.kaya@iste.edu.tr*
[2] *Kocaeli University, Department of Geomatics Engineering, Türkiye, arzu.erener@kocaeli.edu.tr*

Cite this study: Kaya, E., & Erener, A. (2024). UAV-mounted thermal camera and its analysis on urban surface textures. International Journal of Engineering and Geosciences, 9 (1), 49-60

https://doi.org/10.26833/ijeg.1288990

Keywords
Thermal UAV
Remote Sensing
Pearson Correlation
Urban heat
Surface temperature

Research Article

Received:28.04.2023
Revised: 22.05.2023
Accepted:06.06.2023
Published:02.01.2024

Abstract

Temperature increase, especially global warming, can be observed depending on various factors which led to several severe environmental problems. Urban areas are the most effected places by this temperature increase. Urban heat concentration, the so-called heat island effect, is high in structural areas. This situation causes human life to be adversely affected. Therefore, constant measurement and analyses are required to assess outdoor thermal comfort and thermal stress in urban areas. Today, unmanned aerial vehicle (UAV) systems are used as a rapid data production technique in Earth observation activities. Thermal cameras integrated into UAV systems can monitor the temperature values in urban areas precisely and constantly. This study focuses on the potential application of a UAV-mounted thermal camera system at a local scale due to its rapid response to surface temperature variables. A thermal camera UAV system to measure the energy fluxes and temperatures from the earth's surface, which are integral to understanding landscape processes and responses. Thus, UAV thermal sensors were used directly for different land cover types in and around the Faculty of Engineering building of Kocaeli University in Türkiye. Derived UAV surface temperatures were compared with simultaneously acquired in situ temperature measurements. Simultaneous terrestrial temperature measurements were obtained by using TFA ScanTemp 410 model surface temperature meter. A high correlation between UAV surface temperatures and terrestrial measurements was utilized by Pearson correlation with a 0.94 coefficient. It was concluded that the UAV-mounted thermal camera system is a promising tool that has increased opportunities to understand surface temperature variability at high spatial and temporal resolution.

1. Introduction

Increasing impermeable surfaces, destruction of forest areas, urbanization and industrialization contributed to climate change and global warming. Investigating these climate changes and global warming, and creating climate models takes an important place in the estimation and prevention of future environmental damages. The most important soil parameter in these scientific studies is the land surface temperature (LST). The LST is the most important parameter in calculating the energy transfer between the surface and the atmosphere [1]. It can be used in scientific studies related to evapotranspiration, hydrology, climate change, and geothermal energy [2-7].

Generally, the LST is derived from satellite-based thermal infrared (TIR) measurements. Optical remote sensing, however, is limited due to high acquisition costs [8]. Given recent developments in UAVs, thermal images offer the opportunity to measure surfaces in high spatial and temporal resolution at a low cost and this has been explored in recent years by different disciplines for the spatial analysis of surface temperatures [9-15].

They have been compared and analyzed LST data generated by a TIR camera mounted on an UAV and LST data from the Landsat 8 satellite for seven specific periods. They investigated LSTs in green spaces, specifically those of different land cover types in an urban park in Korea [10]. Zengin et al. [16] analyzed thermal camera images and spatial thermal comfort at Ataturk Campus, Türkiye. As a result of the analyzes and evaluations, it was emphasized that the use of natural herbaceous plants is important in terms of providing thermal comfort in urban planning. Gülten and Aksoy

[17] was investigated the heat distribution by the thermal imaging method in a pilot study area of Elazığ, Türkiye. In the study, the thermal behaviors of the building, street, roof, and pavement were evaluated by making surface temperature measurements to investigate the urban heat island (UHI) effect. Yalçıner et al. [18] were examined the structural destructions using thermal imaging, microwave moisture measurements, and building radar systems in the Hagia Sophia Museum, Türkiye. In this way, it was determined whether there was any deterioration on the walls of the Museum. Aerobic stability was evaluated by Ünal et al. [19] with 3 pieces of 500 kg corn and wheat bale silage each obtained from Tekirdag Namık Kemal University application and research farm. As a result of the research, it was concluded that the thermal camera imaging technique can be used as a practical method to evaluate the aerobic stability of silages in laboratory conditions. In the study conducted by Çamoğlu and Genç [20], water stress was determined in green bean plants using spectral reflection data and thermal imaging techniques. The researchers were concluded that water stress can be better explained with thermal indices, especially at the I–100 level, in the classification and regression tree analysis on the sample data sets. In the study, it was determined that the Structural Independent Pigment Index (SIPI) and Normalized Vegetative Change Index (NDVI) from the spectral indices, the plant water stress index (CWSIe) calculated based on the thermal indices, and the plant water stress index (CWSIa) calculated according to the artificial reference surfaces were found in green beans. They have been suggested to be used in the determination of water stress. In the study conducted by Küçüktopcu and Cemek [21], heat loss in poultry houses was monitored with thermal camera data. As a result of the study, it was understood that thermal imaging technology can detect the structural problems that cause heat losses and gains. It was observed that the most heat loss was caused by the gaps in the windows and doors which leads to energy loss in buildings. A solution was sought for the structural problems that cause heat loss in greenhouses by using thermal camera data in Çayli et al. [22]. It has been observed that the places where the heat loss is the most in the greenhouses are the bottom of the doors, the margins, the openings on the edges of the ventilation windows, the roof-front wall, and the side roof wall junctions of the covering material. In the study by Akçay [23], terrestrial photogrammetric analysis was performed using multispectral and thermal cameras. 3D models were produced using images obtained from cameras. Seven control points were used during model production. The model was produced in the point cloud after the production step. In the study conducted by Durgut and Akçay [24], a 3D model of the graphics card was created using thermal camera data. As a result of the study, it was concluded that thermal photogrammetric 3D models can be used to detect problems that may occur during the production and maintenance of electronic products such as computer hardware. In the study conducted by Gülci and Akay [25], the locations of ecological art structures were evaluated using UAV systems and thermal infrared camera data. In the study conducted by Wu et al. [26] in the Jiading Campus area of Tongji University, the LST was calculated using the thermal camera integrated into the UAV. A meteorological ground observation station was used for control purposes. It has been observed that there is a difference between -1.73 and 1.45 Kelvin between the surface temperatures obtained from the terrestrial observation station and UAV systems. Feng et al. [27] calculated the evapotranspiration of various vegetation with the thermal data obtained from UAV systems in a small part of the city of Nanjing, China. As a result of the study, it was observed that high-accuracy evapotranspiration values were obtained with the data obtained from the thermal UAV on different vegetation surfaces. Qin et al. [28] conducted a study in the Beijing University Shenzhen campus area, evapotranspiration was calculated for different vegetation with images obtained by thermal UAV systems and thermal remote sensing data. R^2=0.95, RMSE=30.33 between evapotranspiration obtained from thermal UAV and remote sensing systems. They revealed that thermal UAV systems can be used in the planning of urban areas as a result of statistical analysis. Jiang et al. [29] were taken photographs at different angles with thermal UAV and UAV systems in Nanjing, China. The relationship between the differences between the obtained temperatures and the directions of the buildings has been revealed.

In present study, LSTs of different land cover types were investigated and compared with simultaneous in situ terrestrial temperatures measured by contact thermometers. Surface temperature variability at high spatial and temporal resolution was revealed which could contribute to decision-making for urban spaces and environmental planning in consideration of the thermal environment.

2. Method

2.1. Study Area

Kocaeli city is located in Marmara Region and it is one of the dense industrial provinces of Türkiye through which the D-100 and TEM highways pass through the city. It was mainly a production, storage, and transfer region for more than 1020 industrial institutions in various sectors such as petroleum refineries, automotive, chemistry, textile, machine, food, paper, wood, tanning, coal, etc. Kocaeli's climate constitutes a transition between the Mediterranean and the Black Sea climate. The city center is hot in the summer with low rainfall and mainly rainy and sometimes snowy and cold in winter. The highest temperature measured in the city center is 41.6°C, the lowest temperature is -8.7°C, and the average annual temperature is 14.8°C. The average annual precipitation in Kocaeli exceeds 835 mm. It is the 10th most populous city in Türkiye and the 2nd city in terms of population density. According to 2021 Turkish Statistical Institute (TUIK) data, it has a population of 2.033.441 people. Kocaeli University has its main campus in the borders of Izmit District, in the north-northwest direction of the center of Kocaeli Province. It was established in 1992 with a campus area of 778,466 m^2. Within the campus area, there are forest green areas and

a lake as well as the buildings belonging to the university units. In addition to administrative buildings, there are sports facilities and social areas on the campus. The Engineering Faculty building in Kocaeli University's central campus and its surroundings were defined as the test area (Figure 1).

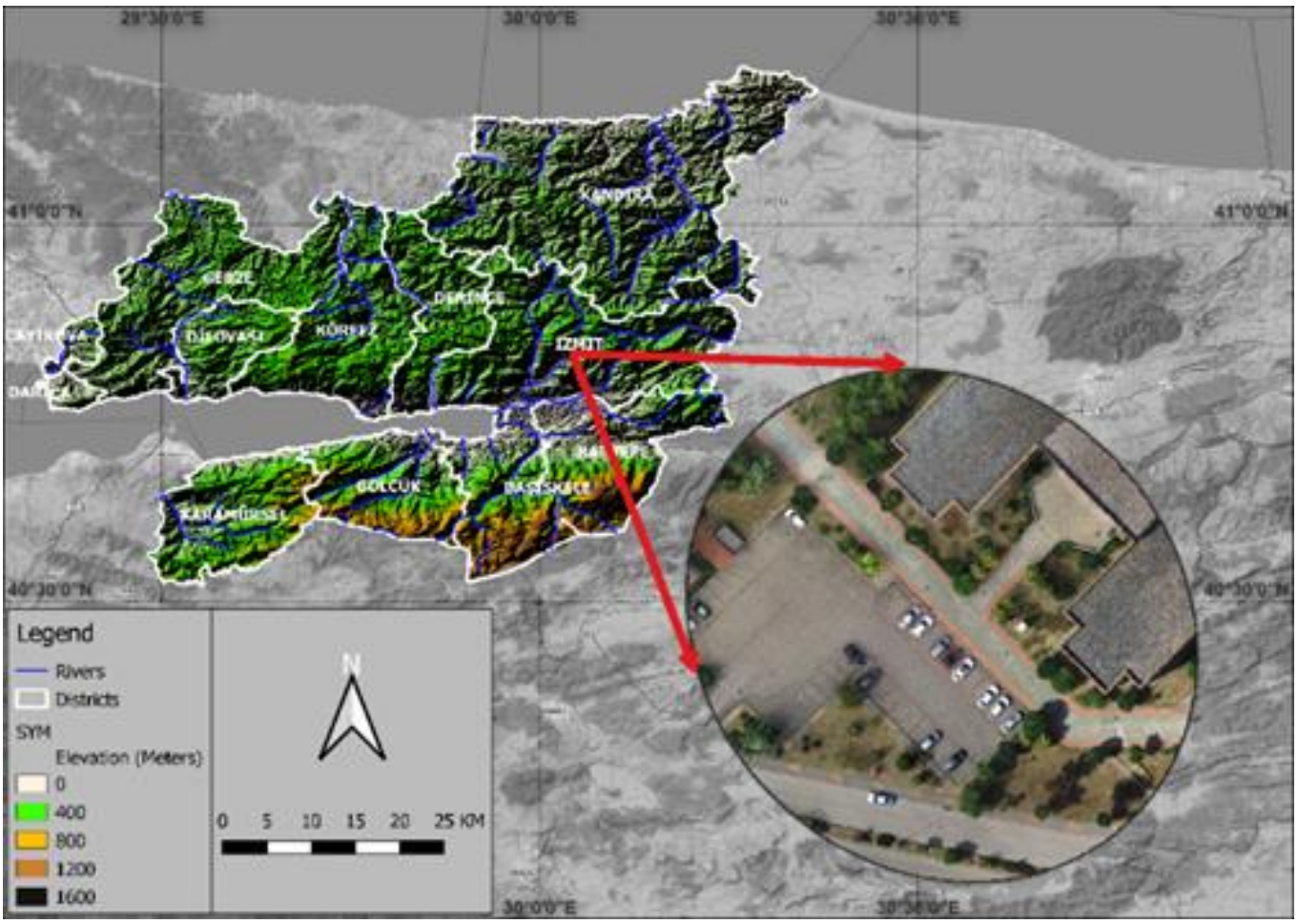

Figure 1. The study area.

The study area is centered at 40°49'23.56" N and 29°55'31.50" E. Instant weather conditions were taken into account in the selection of the study area. The flight operation was carried out on 20 August 2021 between 14.00 - 15.30 LT in the afternoon.

The weather data was additionally obtained from the eleven weather stations from Kocaeli districts. Values such as temperature, humidity, and wind speed were determined as presented in Table 1.

Table 1. Weather data in a period of field measurements.

SI	SN	T	RH	WS	SR
18409	Başiskele	25	55	5.9	96.03
18410	Darıca	26.5	47	6.5	82.25
18411	Dilovası	26.6	56	5.8	100.64
17639	Gebze	25.7	55	5.1	96.38
17067	Gölcük	28.3	50	3.9	0
18104	Kandıra	26.7	55	3.6	91.95
18412	Karamürsel	26.7	46	7.5	92.62
18413	Kartepe	25	56	3.2	96.04
17066	Kocaeli	26.7	80	2.6	0
18414	Körfez	28.5	45	5.1	101.15
19116	Derince	27.4	44	3.6	98.36

SI: Station number, SN: Station name, T: Temperature (°C), RH: Relative humidty (%), WS: Wind speed (m/s), SR: Solar radiation (WH/m²)

2.2. Material

The UAV TIR LST data acquisition process can be divided into LST data collection through UAV TIR image capture and ortho mosaic matching stage, and a survey of ground control points (GCPs) for accurate georeferencing of the LST data [30-39].

Using the Remote Sensing Method to Simulate the Land Change in the Year 2030. Evaluation from Rural to Urban Scale for the Effect of NDVI-NDBI Indices on Land Surface Temperature, in Samsun, Türkiye [40]. The assessment of the thermal behavior of an urban park surface in a dense urban area for planning decisions. Using GIS analysis to assess urban green space in terms of accessibility: case study in Kütahya [41]. Determining the bioclimatic comfort in Kastamonu City. Sustainability of urban coastal area management: A case study on Cide [42]. A geographic information systems and remote sensing–based approach to assess urban micro-climate change and its impact on human health in Bartin, Türkiye [43]. The effects of climate on land use/cover: a case study in Türkiye by using remote sensing data. Investigation of the relationship between bioclimatic comfort and land use by using GIS and RS techniques in Trabzon. Integrating of settlement area in urban and

forest area of Bartin with climatic condition decision for managements.

UAV TIR cameras have lower resolutions compared to red, green, and blue (RGB) and multispectral cameras and single-band images [26]. This study used the Parrot Anafi brand UAV system with the thermal sensor to obtain the surface terminal. The characteristics of UAV with thermal sensors are given in Table 2.

The sample points were collected from the field to control the surface temperature map obtained from the thermal UAV. During the data generation with the UAV simultaneous in situ temperature measurements were applied with the TFA ScanTemp 410 infrared thermometer measuring device (Figure 2 and Figure 3).

The specifications of the TFA ScanTemp 410 Infrared Thermometer surface temperature measuring device are given in Table 3.

Table 2. Parrot Anafi model UAV specifications [44].

Properties	Technical Features
Weight	315 g
Maximum flight time	26 minutes
Maximum horizontal/vertical speed	34 mph / 4 m/s
Maximum wind resistance	31 mph
Max working height	4500 m
Operating temperature	-10 ° C with 40 ° C
Folded size	218x69x64mm
Sensor	CMOS 1 / 2.4 ", 21MP
HDR	4K UHD, 2.7K and 1080p videos, JPEG photos
Photo formats	JPEG, DNG (RAW)
Photo modes	Single, burst, bracketing, timer, and panorama
Maximum video sampling rate	100Mbps
Diaphragm open	f / 2,4
Sensor	FLIR Lepton 3.5 microbolometer (radiometric)
Sensor resolution	160x120
Spectral band	8-14µm
Photo format	JPEG
Photo resolution	3264x2448 (4/3)
Video format	MP4
Video recording resolution	1440x1080, 9fps
Sensibility	±5% max. (High gain) or ±10% max. (Low gain)

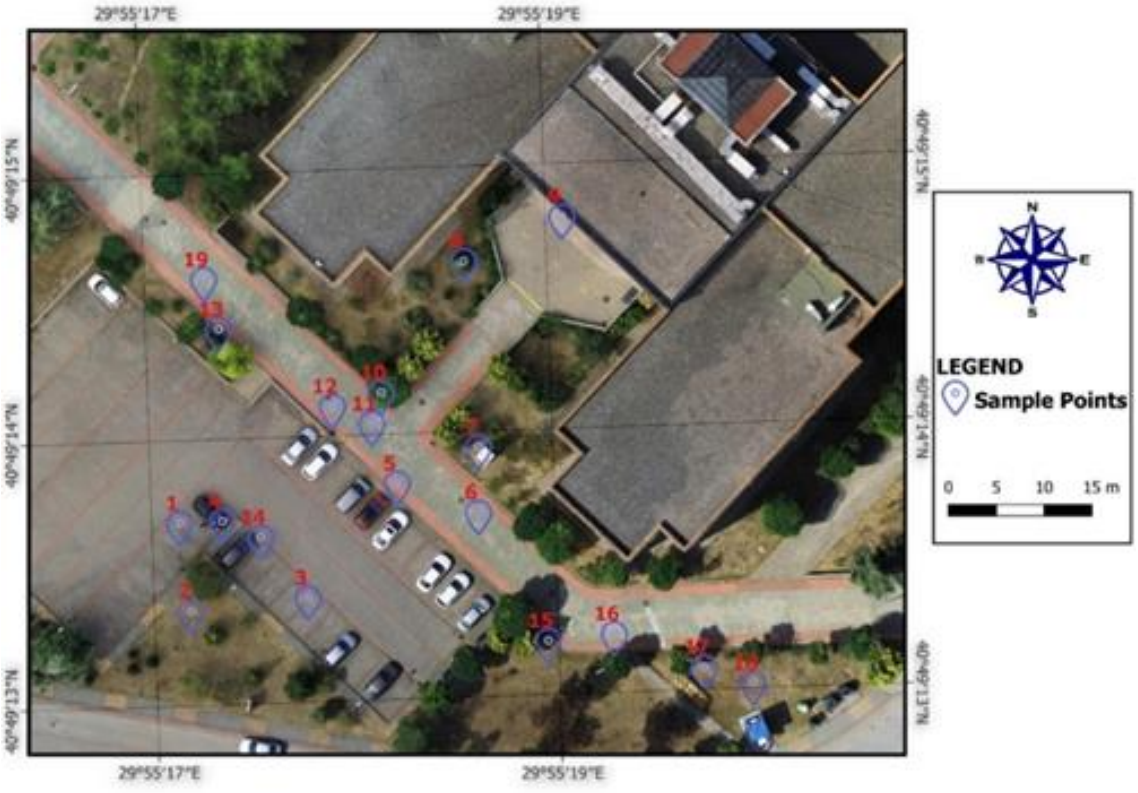

Figure 2. Sample points in the study area.

Figure 3. Measurement at sample points with the TFA ScanTemp 410 Infrared Thermometer.

Table 3. TFA ScanTemp 410 infrared thermometer surface temperature gauge specifications [45].

Properties	Technical Features
Laser temperature measuring range	-60°C +500°C
Laser temperature accuracy	±2°C
ºC/ºF Ability to choose units	Available
Screen resolution	0,1°C
Target rate	11:1
Weight	180 grams
Dimensions	175 x 39 x 80 m
Power source	2 pieces AAA batteries

Using the TFA ScanTemp 410 Infrared Thermometer, temperature measurements were applied to different surface textures in the field. These measurements were accepted as ground truth and the temperature values obtained from the UAV systems were compared with this collected ground in situ database.

2.3. Method

Initially, flight planning was defined to obtain data from the thermal UAV. A flight plan was prepared in Pix4D Capture software and the flight altitude was determined 40 meters. Two different photos were obtained with the RGB camera and the thermal camera on the Anafi Thermal UAV. During the flight, 562 pictures were obtained. In the project, the transverse and longitudinal overlap rate was entered as 90%. The ground sampling interval is 1.34 centimeters. The pictures collected during the flight were stored on the memory card of the aircraft in the Joint Photographic Expert Group (JPEG) format. The images were transferred to the trial version of Pix4D Mapper software. The projection of the project was entered as UTM Zone 35. The photos were initially matched by mounting points throw the images. Approximately 25000 anchor points are assigned per image. After the matching process, the exact coordinates of the photographs were calculated.

In order to create the point cloud, the point cloud setting section was used. In this step, the image scale ½ was chosen to generate the point cloud. The point density was chosen high and the minimum number of image matching was chosen as 3. The point cloud is saved in .las, .laz, .ply, .xyz formats. As a result of the operations, a total of 55503698 points clouds were created (Figure 7). Pix4D Mapper software was also used to create the orthophoto (Figure 4) and DSM (Figure 5). During the orthophoto production, the information from the thermal camera was processed and the surface temperature map of the area was created (Figure 6).

Figure 6 showed that the Engineering Faculty building was in the temperature range of 30-40 °C in general, and some regions in the roof section have a temperature of 40-50 °C. Green areas were in the range of 20-30 °C. Additionally, building shadows have the lowest temperature ranges between 0-20 °C.

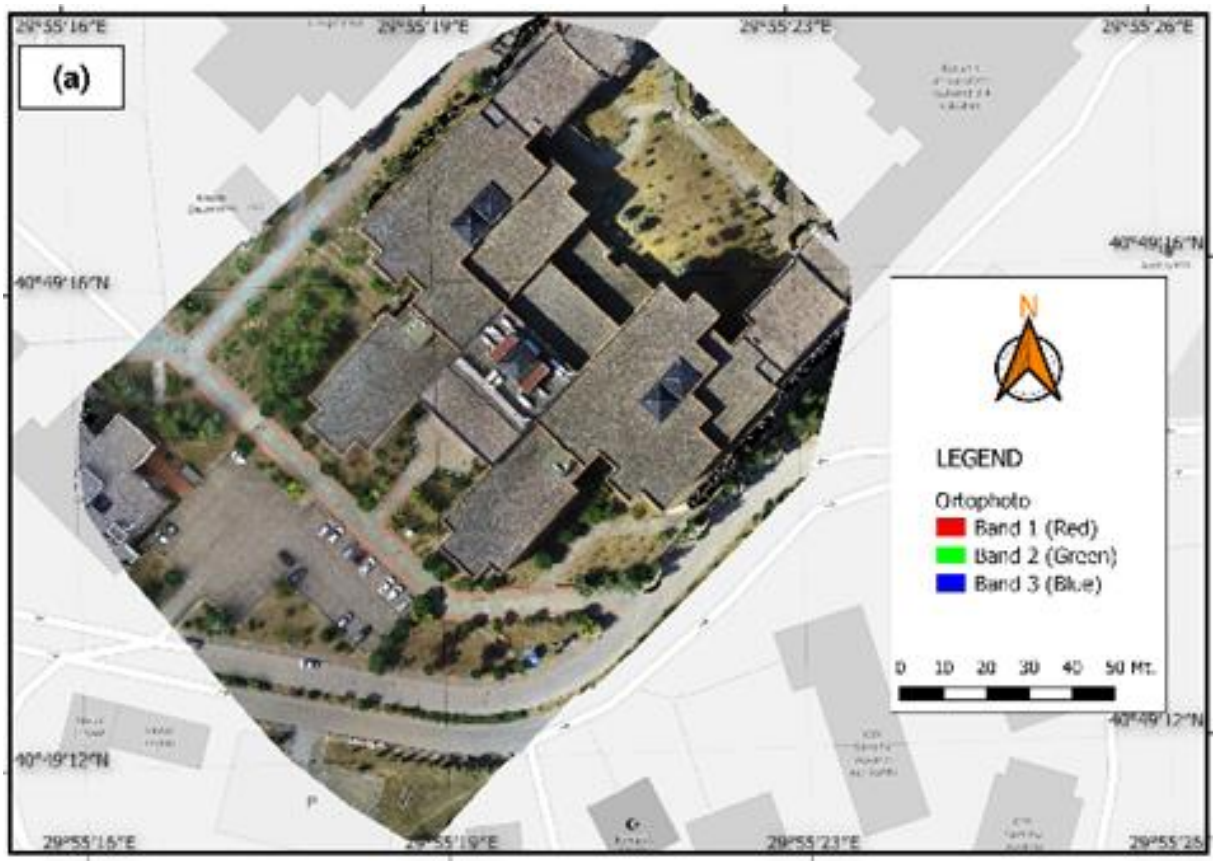

Figure 4. Orthophoto.

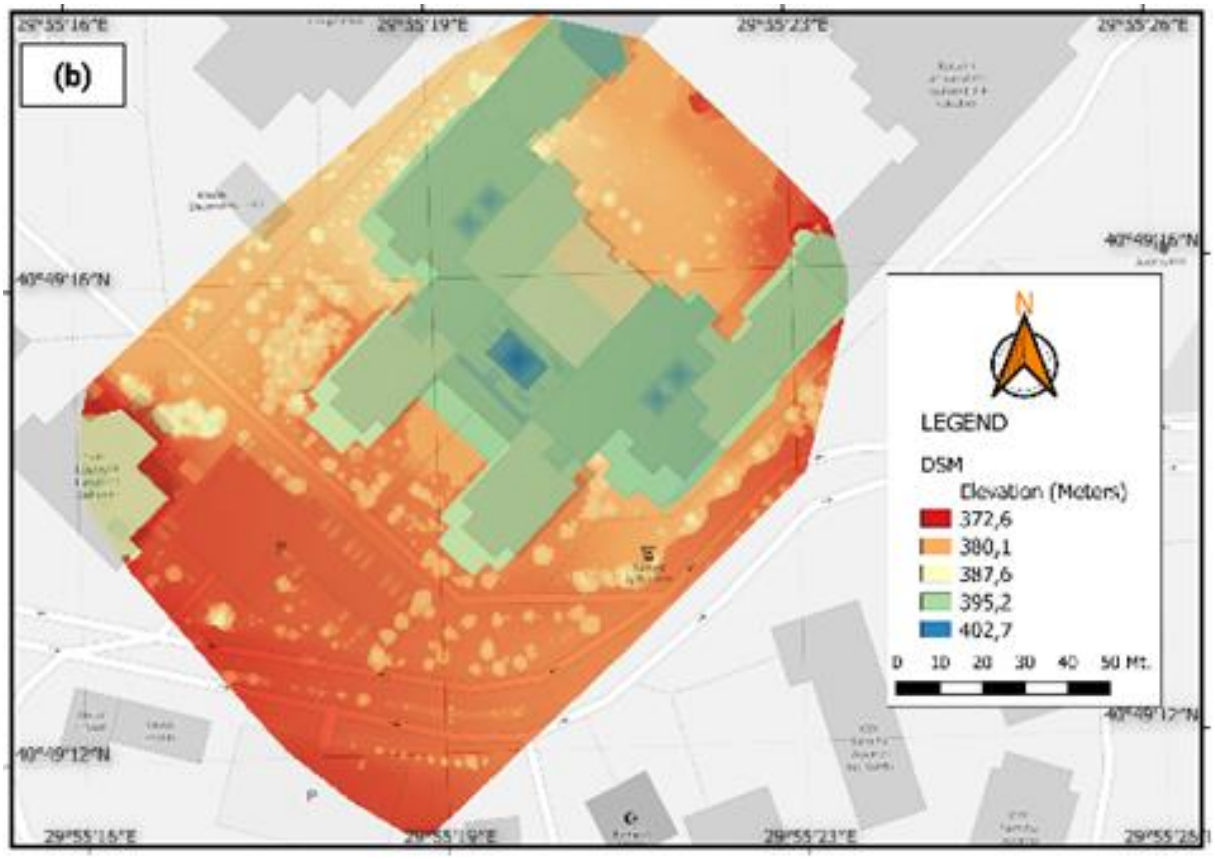

Figure 5. Digital surface model.

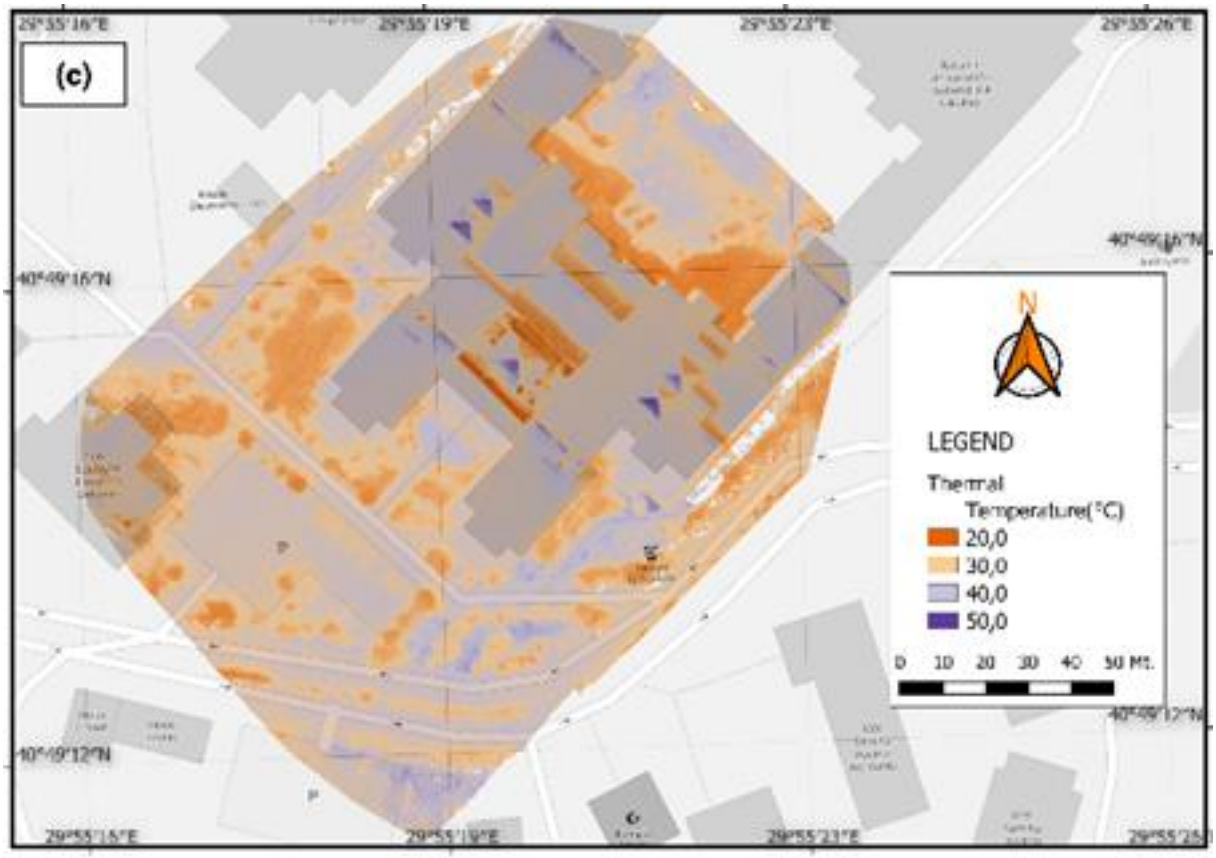

Figure 6. Surface temperature map of the area.

Figure 7. Point cloud.

3. Results

In this study high resolution thermal drone measurements were evaluated in different land cover types and results indicate that there is a wide variability in surface temperature behavior across urban land use types. Additionally, the surface temperatures obtained from the terrestrial observations and UAV systems were compared in order to obtain the performance of UAV thermal measurement performances. In order to evaluate the accuracy of LST data, nineteen LST control points (CP) were selected in the field by considering the land cover type of the study area. The data obtained as a result of the ground measurements and the data obtained from the thermal band are given in Table 4.

The measurement was observed in front of Kocaeli University Engineering Faculty Building on different textures such as key cobblestone, wood, plastic material covered area, and marble area. As a result of the measurements obtained, the differences were examined. The graph of the differences was shown in Figure 8 and Figure 9. It was observed in Table 4 that the difference between values was mostly low and changed between -0.7 to 0.9 °C. There is only one location that indicates a high difference with 5.6 °C due to its location. The flights in this study were obtained from the nadir view.

Therefore, terrestrial measurements coincide to the shadow of any object regions such as building or tree provides higher differences. In this study this measurement was deliberately obtained to represent these differences.

When the points on the soil areas as key cobblestone and marble floor classes are examined, there was not an important difference between the local measurement and the temperature values obtained from the UAV systems. So, when averages of different surfaces are examined for ground measurement, surface temperatures are low in soil areas, while on other surfaces, they are found to be approximately 34,5 °C. While surface temperatures are expected to be low in green areas, at some points the surface temperature is high. This is due to the different surface coverings within the green area surface class. For example, green grass, dry vegetation etc. An average of the data obtained using thermal band is shown to produce results similar to a ground measurement.

The correlation between the temperatures obtained by the Terrestrial measurement method and the Thermal band was shown in Figure 8.

In Figure 9, triangle, circle, and square shapes were used according to the land use types of the points. Gray square-shaped areas indicate green areas. Blue triangles show land areas. Yellow triangles show key cobblestones. The dot with the red square indicates the marble area. The regression line between the points was presented in red. There is a positive correlation between the terrestrial measurement and the temperature values obtained from the thermal band. The correlation coefficient between them was 0.94. This value indicates that there is a high degree of correlation between ground-based and UAV-based measurements.

Table 4. Obtained data and differences between.

TS	SN	GM	TB	D
Green Area	1	32,0	37,6	-5,6
	2	25,3	25,5	-0,2
	3	37,2	37,3	-0,1
	4	38,8	38,0	0,8
Soil Area	5	31,3	31,8	-0,5
	6	27,7	27,4	0,3
Paving Stone Area	7	35,0	35,1	-0,1
	8	36,3	36,4	-0,1
	9	35,2	35,9	-0,7
	10	35,2	35,6	-0,4
	11	37,0	36,2	0,8
	12	33,2	33,5	-0,3
	13	26,0	25,1	0,9
	14	36,5	36,8	-0,3
	15	36,2	35,9	0,3
	16	33,6	33,2	0,4
	17	35,5	35,3	0,2
	18	32,3	32,1	0,2
Marble Ground	19	35,0	34,5	0,5

TS: Texture Surface, SN: Sample Number, GM: Ground Measurement Value (°C), TB: Thermal Band Value (°C), D: Difference (°C)

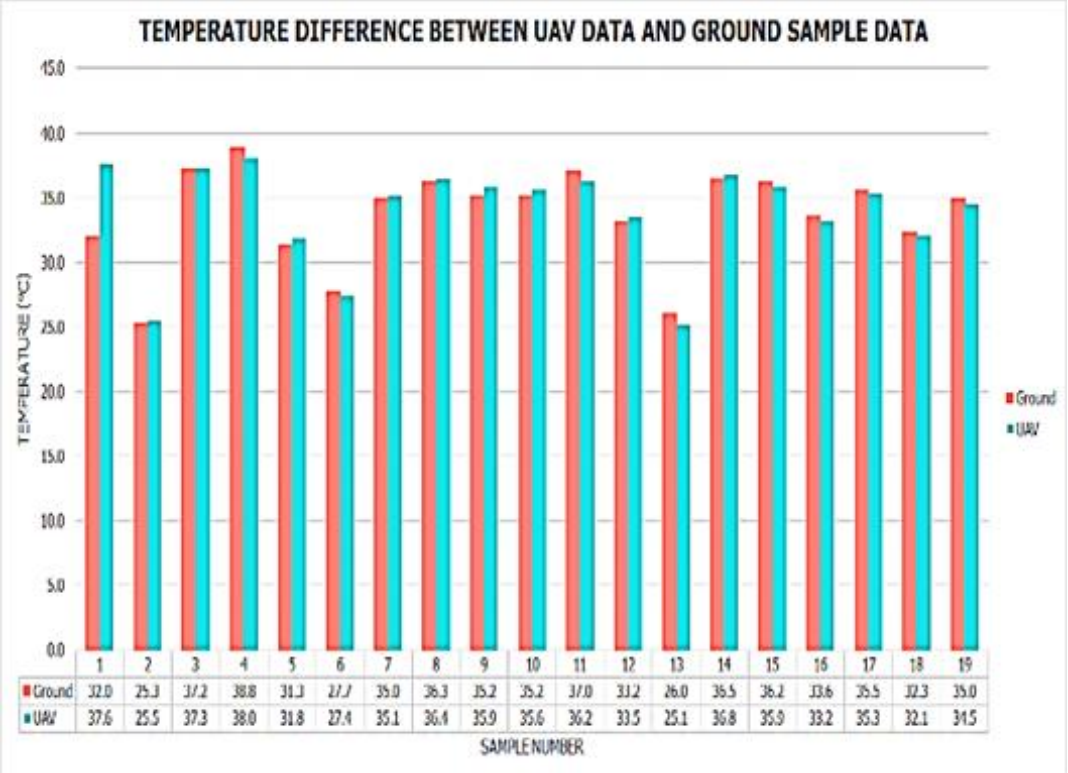

Figure 8. Differences between two different temperature measurements.

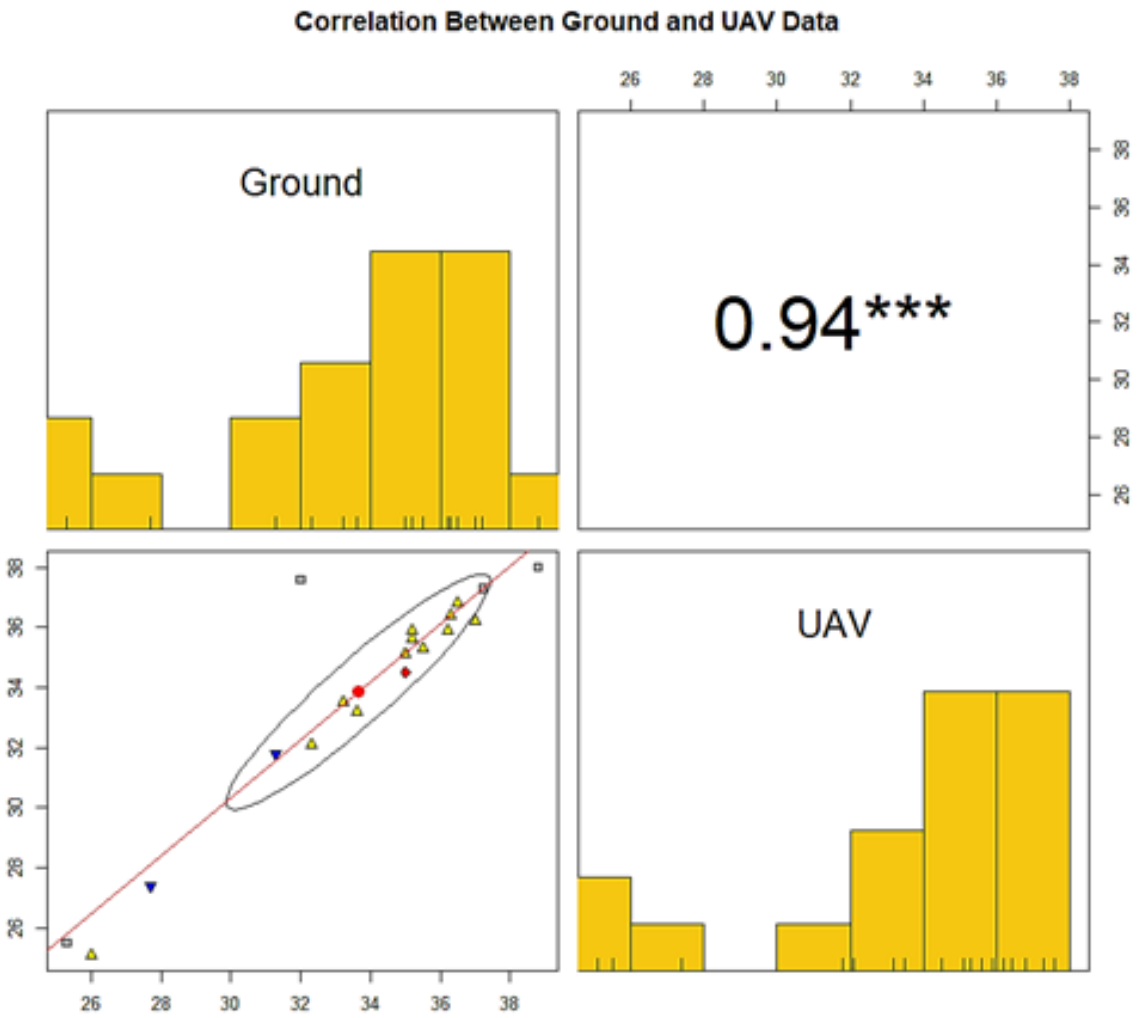

Figure 9. Correlation graph between the temperatures obtained by terrestrial measurement and thermal method.

4. Discussion and Conclusion

The main objectives of this study were to apply drone imagery to capture land surface temperature variability for different surface materials. A thermal camera-integrated UAV system was utilized in this study to evaluate urban surface temperatures. A surface temperature map of approximately 4 ha within the Kocaeli University campus area was monitored. Thermal behaviors of different land surface texture were investigated in the study region. A wide variability between temperature behavior across land use types was obtained. The results indicate that LSTs in different land cover types provide different thermal behaviors such as paving stone area and marble ground temperature were much higher than different vegetation surface types and soil area. This result can lead to the temperatures of different surface textures in urban areas can be easily distinguished by using UAV data.

Additionally, the results indicate that there is a high correlation between UAV-based surface temperatures and simultaneous terrestrial temperature measurements by Pearson correlation with a 0.94 coefficient. There is a difference between -0.7 and 0.9 degrees between the surface temperatures obtained from the terrestrial observation station and UAV systems.

UAVs can cover large areas very quickly, and they can be equipped with tools that can generate RGB, thermal or 3D images. In local areas, UAV systems that can produce fast and instant data compared to the alternative methods. Although UAV systems are fast and instant data generation technique, the most important disadvantage is that they are quickly affected by signal jammers and air conditions such as wind velocity and rain. Especially in city areas, attention should be paid to the UAV during the flight. UAVs can crash due to signal jammers. Since the widespread use of unmanned aerial vehicles is relatively new, legislation related to commercial and recreational use, is still catching up. Despite the disadvantages, it is a technology that can find wide application in many fields.

Acknowledgement

This research was funded by the Scientific Research Project through Kocaeli University, Project No: FDK-2021-2183. Project ID: 2183.

*This article is derived from the Doctoral dissertation titled "Modelling of Bioclimatic Comfort Area Using Artificial Intelligence" conducted under the supervision of Efdal Kaya's Prof. Dr. Arzu Erener.

Thank you for supporting my Doctoral dissertation of Kocaeli University, Scientific Research Projects Office.

Author contributions

Efdal Kaya: Conceptualization, Methodology, Software, Field study Software, Validation **Arzu Erener:** Visualization, Investigation, Writing-Reviewing and Editing.

Conflicts of interest

The authors declare no conflicts of interest.

References

1. Li, Z. L., Tang, B. H., Wu, H., Ren, H., Yan, G., Wan, Z., ... & Sobrino, J. A. (2013). Satellite-derived land surface temperature: Current status and perspectives. Remote Sensing of Environment, 131, 14-37. https://doi.org/10.1016/j.rse.2012.12.008
2. Al Kafy, A., Al Rakib, A., Akter, K. S., Rahaman, Z. A., Jahir, D. M. A., Subramanyam, G., ... & Bhatt, A. (2021). The operational role of remote sensing in assessing and predicting land use/land cover and seasonal land surface temperature using machine learning algorithms in Rajshahi, Bangladesh. Applied Geomatics, 13(4), 793-816. https://doi.org/10.1007/s12518-021-00390-3
3. Aneesha Satya, B., Shashi, M., & Deva, P. (2020). Future land use land cover scenario simulation using open source GIS for the city of Warangal, Telangana, India. Applied Geomatics, 12, 281-290. https://doi.org/10.1007/s12518-020-00298-4
4. Gabriele, M., Brumana, R., Previtali, M., & Cazzani, A. (2023). A combined GIS and remote sensing approach for monitoring climate change-related land degradation to support landscape preservation and planning tools: The Basilicata case study. Applied Geomatics, 15(3), 497-532. https://doi.org/10.1007/s12518-022-00437-z
5. Hoque, I., & Lepcha, S. K. (2020). A geospatial analysis of land use dynamics and its impact on land surface temperature in Siliguri Jalpaiguri development region, West Bengal. Applied Geomatics, 12(2), 163-178. https://doi.org/10.1007/s12518-019-00288-1
6. Moisa, M. B., & Gemeda, D. O. (2021). Analysis of urban expansion and land use/land cover changes using geospatial techniques: a case of Addis Ababa City, Ethiopia. Applied Geomatics, 13(4), 853-861. https://doi.org/10.1007/s12518-021-00397-w
7. Ndossi, M. I., & Avdan, U. (2016). Inversion of land surface temperature (LST) using Terra ASTER data: a comparison of three algorithms. Remote Sensing, 8(12), 993. https://doi.org/10.3390/rs8120993
8. Khanal, S., Fulton, J., & Shearer, S. (2017). An overview of current and potential applications of thermal remote sensing in precision agriculture. Computers and Electronics in Agriculture, 139, 22-32. https://doi.org/10.1016/j.compag.2017.05.001
9. Kraaijenbrink, P. D. A., Shea, J. M., Pellicciotti, F., De Jong, S. M., & Immerzeel, W. W. (2016). Object-based analysis of unmanned aerial vehicle imagery to map and characterise surface features on a debris-covered glacier. Remote Sensing of Environment, 186, 581-595. https://doi.org/10.1016/j.rse.2016.09.013
10. Kim, D., Yu, J., Yoon, J., Jeon, S., & Son, S. (2021). Comparison of accuracy of surface temperature images from unmanned aerial vehicle and satellite for precise thermal environment monitoring of urban parks using in situ data. Remote Sensing, 13(10), 1977. https://doi.org/10.3390/rs13101977
11. Tiwari, A., Sharma, S. K., Dixit, A., & Mishra, V. (2021). UAV remote sensing for campus monitoring: a comparative evaluation of nearest neighbor and rule-based classification. Journal of the Indian Society of Remote Sensing, 49, 527-539. https://doi.org/10.1007/s12524-020-01268-4
12. Polat, N., & Uysal, M. (2018). An experimental analysis of digital elevation models generated with Lidar Data and UAV photogrammetry. Journal of the Indian Society of Remote Sensing, 46(7), 1135-1142. https://doi.org/10.1007/s12524-018-0760-8
13. Sharma, M., Raghavendra, S., & Agrawal, S. (2021). Development of an open-source tool for UAV photogrammetric data processing. Journal of the Indian Society of Remote Sensing, 49, 659-664. https://doi.org/10.1007/s12524-020-01237-x
14. Das, S., & Jain, G. V. (2022). Assessment and prediction of urban expansion using CA-based SLEUTH urban growth model: A case study of Kolkata Metropolitan area (KMA), West Bengal, India. Journal of the Indian Society of Remote Sensing, 50(12), 2277-2302. https://doi.org/10.1007/s12524-022-01602-y
15. Vinod, P. V., Trivedi, S., Hebbar, R., & Jha, C. S. (2023). Assessment of Trees Outside Forest (TOF) in Urban Landscape Using High-Resolution Satellite Images and Deep Learning Techniques. Journal of the Indian Society of Remote Sensing, 51(3), 549-564. https://doi.org/10.1007/s12524-022-01646-0
16. Zengin, M., Yilmaz, S., & Mutlu, B. E. (2019). Atatürk University Campus in terms of spatial thermal comfort analysis of thermal camera images. Atatürk Üniversitesi Ziraat Fakültesi Dergisi/Atatürk University Journal of Agricultural Faculty, 50(3), 239-247. https://doi.org/10.17097/ataunizfd.535209
17. Gülten, A. A., & Aksoy, U. T. (2011). Kentsel bir alanda ısı dağılımının termal görüntüleme yöntemiyle incelenmesi. Engineering Sciences, 6(4), 1582-1589.
18. Yalçıner, C. Ç., Gündoğdu, E., Kurban, Y. C., & Altunel, E. (2017). Eski Eserlerdeki Yapısal Tahribatların Termal Görüntüleme ve Mikrodalga Nem Ölçümleri ile Belirlenmesi: Ayasofya Müzesi Örnek Çalışması. Çanakkale Onsekiz Mart Üniversitesi Fen Bilimleri Enstitüsü Dergisi, 3(2), 34-47. https://doi.org/10.28979/comufbed.346240
19. Ünal, Ö., Koc, F., Okur, A. A., Okur, E., & Özdüven, M. L. (2018). Using thermal imaging camera technique to evaluation of the aerobic stability of corn and wheat silage. Alınteri Journal of Agriculture Science, 33(1), 55-63.
20. Çamoğlu, G., & Genç, L. (2013). Taze Fasulyede Su Stresinin Belirlenmesinde Termal Görüntülerin ve Spektral Verilerin Kullanımı. COMU Journal of Agriculture Faculty, 1(1), 15-27.

21. Küçüktopcu, E., & Cemek, B. (2020). Kümeslerdeki ısı kayıplarının termal kamerayla izlenmesi. Anadolu Tarim Bilimleri Dergisi, 35(3), 404-409. https://doi.org/10.7161/omuanajas.758342
22. Çayli, A., Akyüz, A. D. İ. L., Baytorun, A. N., Üstün, S., & Boyaci, S. (2016). Determination of structural problems causing heat loss with the thermal camera in greenhouses. Kahramanmaraş Sütçü İmam Üniversitesi Doğa Bilimleri Dergisi, 19(1), 5-14.
23. Akçay, Ö. (2021). Photogrammetric analysis of multispectral and thermal close-range images. Mersin Photogrammetry Journal, 3(1), 29-36.
24. Durgut, A., & Akçay, Ö. (2016). Termal kamera ile ekran kartının 3 boyutlu modelinin oluşturulması. Anadolu University Journal of Science and Technology A-Applied Sciences and Engineering, 17(1), 51-63. https://doi.org/10.18038/btda.72883
25. Gulci, S., & Akay, A. E. (2016). Using thermal infrared imagery produced by unmanned air vehicles to evaluate locations of ecological road structures. Journal of the Faculty of Forestry-Istanbul University. 66(2), 698-709. http://dx.doi.org/10.17099/jffiu.76461
26. Wu, Y., Shan, Y., Lai, Y., & Zhou, S. (2022). Method of calculating land surface temperatures based on the low-altitude UAV thermal infrared remote sensing data and the near-ground meteorological data. Sustainable Cities and Society, 78, 103615. https://doi.org/10.1016/j.scs.2021.103615
27. Feng, L., Liu, Y., Zhou, Y., & Yang, S. (2022). A UAV-derived thermal infrared remote sensing three-temperature model and estimation of various vegetation evapotranspiration in urban micro-environments. Urban Forestry & Urban Greening, 69, 127495. https://doi.org/10.1016/j.ufug.2022.127495
28. Qin, L., Yan, C., Yu, L., Chai, M., Wang, B., Hayat, M., ... & Qiu, G. Y. (2022). High-resolution spatio-temporal characteristics of urban evapotranspiration measured by unmanned aerial vehicle and infrared remote sensing. Building and Environment, 222, 109389. https://doi.org/10.1016/j.buildenv.2022.109389
29. Jiang, L., Zhan, W., Tu, L., Dong, P., Wang, S., Li, L., ... & Wang, C. (2022). Diurnal variations in directional brightness temperature over urban areas through a multi-angle UAV experiment. Building and Environment, 222, 109408. https://doi.org/10.1016/j.buildenv.2022.109408
30. Kim, D., Yu, J., Yoon, J., Jeon, S., & Son, S. (2021). Comparison of accuracy of surface temperature images from unmanned aerial vehicle and satellite for precise thermal environment monitoring of urban parks using in situ data. Remote Sensing, 13(10), 1977. https://doi.org/10.3390/rs13101977
31. Ağca, M., Gültekin, N., & Kaya, E. (2020). İnsansız hava aracından elde edilen veriler ile kaya düşme potansiyelinin değerlendirilmesi: Adam Kayalar örneği, Mersin. Geomatik, 5(2), 134-145. https://doi.org/10.29128/geomatik.595574
32. Ulvi, A. (2018). Analysis of the utility of the unmanned aerial vehicle (UAV) in volume calculation by using photogrammetric techniques. International Journal of Engineering and Geosciences, 3(2), 43-49. https://doi.org/10.26833/ijeg.377080
33. Ulvi, A., & Toprak, A. S. (2016). Investigation of three-dimensional modelling availability taken photograph of the unmanned aerial vehicle; sample of kanlidivane church. International Journal of Engineering and Geosciences, 1(1), 1-7. https://doi.org/10.26833/ijeg.285216
34. Yakar, M., & Doğan, Y. (2017). Mersin Silifke Mezgit Kale Anıt Mezarı fotogrametrik rölöve alımı ve üç boyutlu modelleme çalışması. Geomatik, 2(1), 11-17. https://doi.org/10.29128/geomatik.296763
35. Şasi, A., & Yakar, M. (2018). Photogrammetric modelling of hasbey dar'ülhuffaz (masjid) using an unmanned aerial vehicle. International Journal of Engineering and Geosciences, 3(1), 6-11. https://doi.org/10.26833/ijeg.328919
36. Kusak, L., Unel, F. B., Alptekin, A., Celik, M. O., & Yakar, M. (2021). Apriori association rule and K-means clustering algorithms for interpretation of pre-event landslide areas and landslide inventory mapping. Open Geosciences, 13(1), 1226-1244. https://doi.org/10.1515/geo-2020-0299
37. Alptekin, A., & Yakar, M. (2021). 3D model of Üçayak Ruins obtained from point clouds. Mersin Photogrammetry Journal, 3(2), 37-40. https://doi.org/10.53093/mephoj.939079
38. Mirdan, O., & Yakar, M. (2017). Tarihi eserlerin İnsansız Hava Aracı ile modellenmesinde karşılaşılan sorunlar. Geomatik, 2(3), 118-125. https://doi.org/10.29128/geomatik.306914
39. Ulvi, A., Yakar, M., Yiğit, A. Y., & Kaya, Y. (2020). İha ve Yersel Fotogrametrik Teknikler Kullanarak Aksaray Kızıl Kilisenin 3B Modelinin ve Nokta Bulutunun Elde Edilmesi. Geomatik, 5(1), 19-26. https://doi.org/10.29128/geomatik.560179
40. Degerli, B., & Çetin, M. (2022). Evaluation from rural to urban scale for the effect of NDVI-NDBI indices on land surface temperature, in Samsun, Türkiye. Turkish Journal of Agriculture-Food Science and Technology, 10(12), 2446-2452. https://doi.org/10.24925/turjaf.v10i12.2446-2452.5535
41. Cetin, M. (2015). Using GIS analysis to assess urban green space in terms of accessibility: case study in Kutahya. International Journal of Sustainable Development & World Ecology, 22(5), 420-424. https://doi.org/10.1080/13504509.2015.1061066
42. Cetin, M. (2016). Sustainability of urban coastal area management: A case study on Cide. Journal of Sustainable Forestry, 35(7), 527-541. https://doi.org/10.1080/10549811.2016.1228072
43. Zeren Cetin, I., Varol, T., & Ozel, H. B. (2023). A geographic information systems and remote sensing–based approach to assess urban micro-climate change and its impact on human health in Bartin, Turkey. Environmental Monitoring and Assessment, 195(5), 540. https://doi.org/10.1007/s10661-023-11105-z

44. Zeren Cetin, I., & Sevik, H. (2020). Investigation of the relationship between bioclimatic comfort and land use by using GIS and RS techniques in Trabzon. Environmental Monitoring and Assessment 192, 1-14. https://doi.org/10.1007/s10661-019-8029-4

45. https://www.paksoyteknik.com.tr/paksoy-topcon/iha/parrot-anafi-thermal.html